RSC Advances

PAPER

View Article Online
View Journal | View Issue

Cite this: *RSC Adv.*, 2025, **15**, 36213

Simultaneous conversion of dialkyl phosphites to dialkyl phosphoric acids and SeO_2 to Se nanoparticles in water and their anticancer properties

Babak Kaboudin, *[a] Hesam Esfandiari,[a] Ali Sabzalipour,[a] Zahra Oushyani Roudsari,[b] Fahimeh Varmaghani,[a] Tianjian Zhang[c] and Yanlong Gu[c]

Received 12th July 2025
Accepted 15th September 2025

DOI: 10.1039/d5ra04981d

rsc.li/rsc-advances

A novel, very simple, one-way, economical, and convenient reaction method for the simultaneous synthesis of dialkyl phosphoric acids and selenium nanoparticles has been developed. This communication describes the synthesis and characterization of selenium nanoparticles through the reactions of dialkyl phosphites and selenium dioxide. Dialkyl phosphites serve as reducing agents for converting selenium dioxide (a hazardous selenium source) to selenium nanoparticles (Se NPs), and conversely, selenium dioxide oxidizes dialkyl phosphites to dialkyl phosphoric acids. The impact of solvents, temperature, and ratio of materials is included in this study. Most of the prepared Se NPs tend to agglomerate, and their stability improved by the addition of β-cyclodextrin. In addition to enhancing the stability of Se NPs by cyclodextrin, the anticancer properties of the as-prepared Se NPs stabilized by β-cyclodextrin are studied. The reported method presents the conversion of selenium dioxide (a hazardous selenium source) to valuable Se NPs (hemispherical Se crystals) and industrially applicable dialkyl phosphoric acids from inexpensive materials with zero E factor and one atom economy.

Introduction

The development of safe, efficient, and economical synthesis methods is one of the main challenges for chemists.[1–3] Over the past two decades, green and economical methods for the synthesis of organic and inorganic compounds have attracted increasing attention due to increasing environmental problems.[4–6] Selenium (Se) is a very important element in the fields of biology, physics, and chemistry, with many applications, both industrially and commercially.[7–9] The elemental form of selenium is insoluble in water. Among the four oxidation states of selenium that exist in nature (6, 4, 2, and 0), elemental selenium is the least toxic and plays a critical role in the maintenance of human health and growth.[10] In nanotechnology, the synthesis of metal nanoparticles is important due to their applications in biomedicine.[11] Amongst the various metal nanoparticles, selenium nanoparticles (Se NPs) have attracted much attention due to their antimicrobial,[12] antioxidant,[13] anticancer,[14] and anti-biofilm properties.[15] On the other hand, according to literature reports, Se NPs are extensively used in semiconductors, renewable energy devices, and photocells.[16] Various physical (UV irradiation, laser ablation, and hydrothermal),[17] chemical,[18] and biological[19] methods have been reported for the synthesis of Se NPs. However, all the methods have a very low atom economy, resulting in the formation of a lot of wastes.

Organophosphorus esters are important materials that have large applications in agricultural, medicinal, industrial, and organic synthesis.[20–22] Among the organophosphorus esters, dialkyl phosphoric acids have attracted much attention due to their use in the oil industry and for the extraction of rare metals.[23–25] For example, bis(2-ethylhexyl) phosphate (D2EHPA, P204) is a famous rare-metal extractant.[26] Dialkyl phosphoric acids have been synthesized by various methods, including the reaction of $POCl_3$ with a long chain alcohol in benzene, followed by alkaline hydrolysis[27] and the reaction of *o*-phenylene phosphorochloridate with alcohols (with more than four carbons in the alkyl group), followed by deprotection of the resulting dialkyl *o*-hydroxyphenyl phosphate with $PhI(OAc)_2$.[28] The first method gives low yields (11–35%) because of the selective crystallization of the solid dialkyl phosphate from the reaction mixture, and it is not applicable for alcohols with less than ten carbons in the alkyl group.

The most common selenium sources for the synthesis of Se NPs are sodium selenite, sodium selenate, selenous acid, sodium selenosulphate, and 1,2,3-selenadiazole. Selenium in

[a]*Department of Chemistry, Institute for Advanced Studies in Basic Sciences, Gava Zang, Zanjan, 45137-66731, Iran. E-mail: kaboudin@gmail.com; kaboudin@iasbs.ac.ir*
[b]*Department of Medical Biotechnology, School of Medicine, Zanjan University of Medical Sciences, Zanjan, Iran*
[c]*School of Chemistry and Chemical Engineering, Huazhong University of Science & Technology, Wuhan 430074, China*

selenite and selenate forms has a hazardous effect even at extremely low concentrations. In order to avoid the use of hazardous selenium sources and additives (reductants and stabilizers) for the synthesis of Se NPs, a direct, atom-efficient, and simple transformation of SeO_2 into Se NPs is necessary. Although the application of SeO_2 for the oxidation of a wide range of organic materials is being investigated,[29,30] the direct synthesis of industrially important dialkyl phosphoric acid compounds through the reaction of SeO_2 and dialkyl phosphites (which is easily prepared from P_4)[24] has not yet been studied. Here, we describe a convenient, one-step process for the synthesis of valuable Se NPs (hemispherical crystalline selenium) and industrially applicable dialkyl phosphoric acids from inexpensive materials with zero E factor, one-atom economy, and complete conversion conditions suitable for scale-up.

Results and discussion

Our continued interest in the green synthesis of organophosphorus compounds motivated us to explore the possibility of synthesizing dialkyl phosphoric acids from dialkyl phosphites in the presence of SeO_2. Diethyl phosphite **1a** was selected as a model compound, and optimization of the reaction conditions was carried out in various solvents (Table S1; the reaction yield was monitored by ^{31}P NMR). In the presence of SeO_2, compound **1a** was converted to diethyl phosphoric acid **2a** in 90% yield in acetonitrile at RT for 12 h. During the reaction, black selenium particles appeared in the reaction mixture. Replacing acetonitrile with other solvents, such as dioxane, DMSO, methanol, toluene, and water, resulted in good to excellent yields. Furthermore, operating the reaction at RT for 3 h in water led to the targeted product **2a** in quantitative yield (Scheme 1). The effect of the amount of SeO_2 on the synthesis of compound **2a** was also examined. Decreasing the amount of SeO_2 to 0.5 equivalent also gave **2a** in quantitative yield. However, a further decrease in the amount of SeO_2 to 0.25 equivalent, resulted in compound **2a** in 45% yield. Further studies showed that the reaction atmosphere had no effect on the yield of the product **2a.** It should be noted that the reaction failed using other selenium sources such as sodium selenite (Na_2SeO_3).

With the optimized conditions in hand, the reaction between various dialkyl phosphites and SeO_2 in water at RT was evaluated (Table 1). It should be noted that dialkyl phosphites with a short chain of alkyl groups gave the corresponding dialkyl phosphoric acids; for instance, the readily hydrolysable dimethyl phosphite gave dimethyl phosphoric acid [$(MeO)_2P(O)OH$, **2b**] in 92% yield. Dialkyl phosphites with primary alkyl chains, such as *n*-butyl, gave the corresponding dialkyl phosphoric acid **2c** in 85% yield. β-substituted aliphatic primary alkyl chains, such as 2-methylpropyl and 2-ethylhexyl, afforded the corresponding products **2d** and **2e** in 90% and 71% yields, respectively. It should be noted that bis(2-ethylhexyl) phosphoric acid (D2EHPA, **2e**), a known rare-metal extractant, was obtained in high purity and yield using this method.

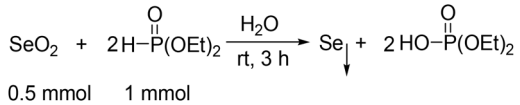

Scheme 1 Reaction of SeO_2 with diethyl phosphite.

Table 1 Reaction of SeO_2 with dialkyl phosphites and diaryl phosphine oxides[a]

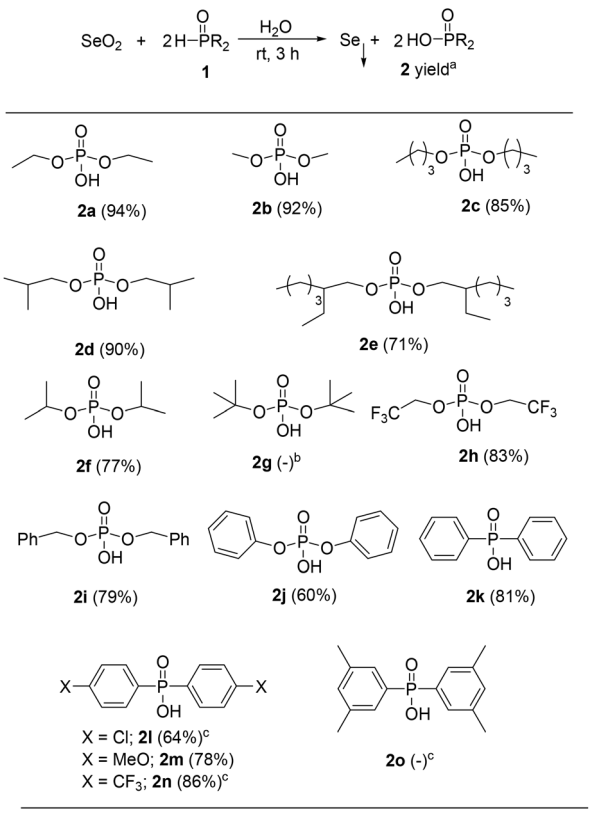

[a] Yields refers to isolated compound **2** for the reaction of **1** (1 mmol) with SeO_2 (0.5 mmol) in water (2 mL). [b] Compound **1g** decomposed in the reaction condition. [c] The reaction was carried out using acetonitrile as the solvent.

Linear secondary alkyl chains, such as *iso*-propyl, performed well in the reaction with a good yield. Although di-*t*-butyl phosphite **1g** didn't give the corresponding phosphoric acid **2g** in this condition or *via* the use of acetonitrile as the solvent, the reaction with di-2,2,2-trifluoroethyl phosphite gave the desired product **2h** in 83% yield. In spite of the lower stability of dibenzyl- and diphenyl-phosphite **1i** and **1j** in water, reaction with SeO_2 in water gave corresponding phosphoric acids **2i** and **2j** in 79% and 60% yields, respectively. In addition, some diaryl phosphine oxides were examined for these transformations. Treatment of diphenyl phosphine oxide with SeO_2 in water gave diphenyl phosphinic acid **2k** in quantitative yield. Various diphenyl phosphine oxide derivatives bearing electron-donating or electron-withdrawing groups on the phenyl moiety in the presence of SeO_2 afforded the corresponding diphenyl phosphinic acids **2l–2n** in good yields. Under similar conditions, di-

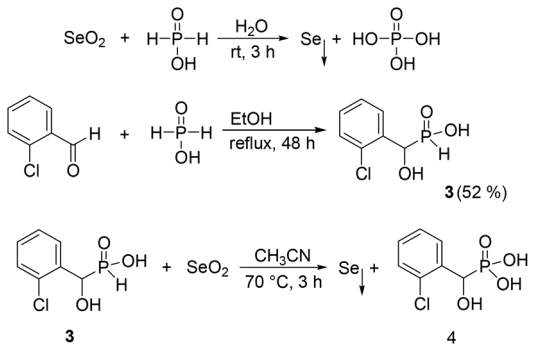

Scheme 2 Reaction of SeO_2 with H_3PO_2 (50%) and compound **3**.

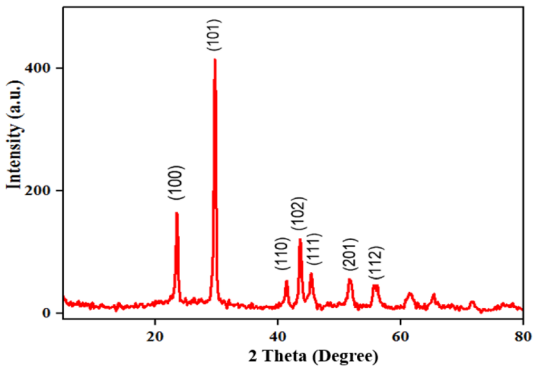

Fig. 2 XRD pattern of DMP-Se NPs.

3,5-dimethyl phosphine oxide **1o**, as a two substituted diaryl phosphine oxide, served as a suitable reaction component; the corresponding product **2o** was obtained without any problems. In all the experiments, Se particles were obtained and collected.

In the next attempt, the conversion of SeO_2 to Se particles was examined in the presence of H_3PO_2 (50%). Interestingly, it was found that treatment of SeO_2 with H_3PO_2 (50%) at RT for 3 h gave Se particles in quantitative yield (Scheme 2).

1-Hydroxy-(2-chlorophenyl)methylphosphinic acid **3** was obtained on a gram scale from the reaction of an aldehyde with hypophosphorus acid at reflux in ethanol for 48 h (Scheme 2), following a literature procedure. Treatment of compound **3** with SeO_2 at 70 °C for 3 h gave the corresponding 1-hydroxyphosphonic acid **4** in 90% yield (Scheme 2).

To obtain information on the size and morphology of Se particles, all the collected samples were subjected to TEM analysis. TEM analysis of the Se particles revealed that the majority of particles agglomerated in all the samples (for example, see Fig. S50 in SI), except Se particles (DMP-Se NPs) collected from the reaction of SeO_2 with dimethyl phosphite (**1b**). As shown in the TEM image (Fig. 1 and S46 in SI), Se particles are clearly visible as hemispherical Se crystals. It should be noted that this sample also tended to aggregate into larger particles.

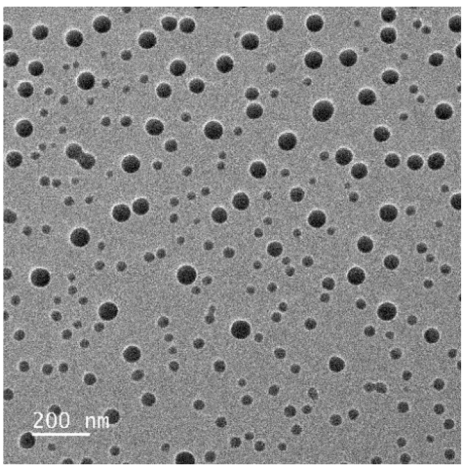

Fig. 1 TEM micrograph of DMP-Se NPs.

The particle size distribution from the TEM micrographs revealed that particle sizes were 25–60 nm (Fig. S47; particle size distribution diagram of DMP-Se NPs). XRD pattern of DMP-Se NPs is shown in Fig. 2, which confirmed the high crystallinity of DMP-Se NPs. The average particle size of DMP-Se NPs was calculated using the Scherrer equation and was found to be 40 nm.

Furthermore, corresponding to the color change of the reaction mixture from colorless to red, formation of Se NPs was confirmed by a sharp absorbance peak of the Se nanoparticles at 265 nm (Fig. S47). XPS spectrum of DMP-Se NPs is shown in Fig. S48. The XPS spectrum of Se revealed a binding energy of 55.18 eV for the purified selenium nanoparticles, confirming the presence of elemental selenium (Se0). The XPS spectrum of oxygen showed broad peaks, indicating the presence of different chemical states of oxygen. The O 1s peaks at 530.6–530.9 eV were attributed to the non-bridging oxygen in the phosphate group (P═O).[31]

The peak at 532.5–535.9 eV was assigned to the combined effects of singly bonded oxygen (–O–) in C–O–P groups, chemisorbed oxygen and oxygen in water.[32] In Fig. S48, the XPS spectrum of phosphorous shows peaks at 132.9–133.1 and 136 eV, which are attributed to tetra-coordinated phosphorus.[33]

As mentioned, TEM analysis showed that in the reaction media, the prepared Se NPs start to aggregate and form larger particles. In continuation to our efforts and literature reports on the synthesis of metal nanoparticles stabilized by cyclodextrins,[34] synthesis of Se NPs was examined in the presence of β-cyclodextrin as a stabilizing agent to prevent aggregation. It was found that the reaction of SeO_2 with diethyl phosphite in water at 60 °C for 2 h in the presence of β-cyclodextrin gave Se NPs without aggregation. The reaction mixture changed its color in 2 h upon adding β-cyclodextrin (Fig. 3). The reaction was also examined in the presence of other stabilizers such as poly(ethyl methacrylate), chitosan, and poly sorbet. Experimental results showed that other stabilizers did not prevent aggregation (Fig. S55).

The formation of non-aggregated Se NPs was confirmed by FE-SEM analysis. As shown in the FE-SEM image (Fig. S49 in SI), Se particles were clearly visible as hemispherical structures.

Furthermore, the anticancer properties of the β-cyclodextrin-stabilized Se NPs (β-CD@SeNPs) were studied (all biological

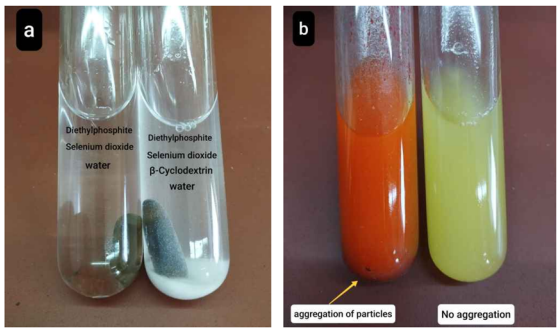

Fig. 3 (a) Reaction mixture of SeO_2 (0.5 mmol) and diethyl phosphite (1 mmol) with and without β-cyclodextrin (0.5 mmol) in water. (b) Corresponding change in the mixture color after 2 h at 60 °C.

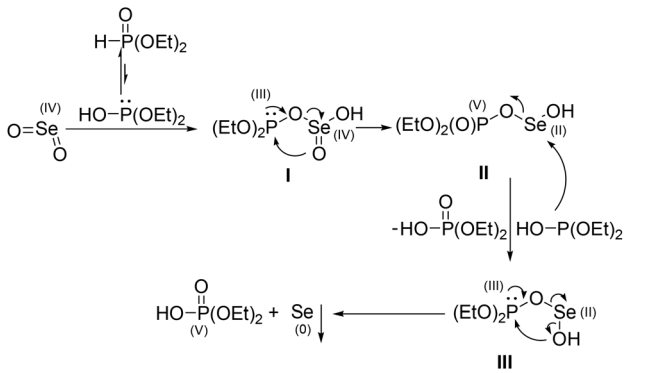

Scheme 3 Proposed reaction mechanism.

samples were purchased from the Iranian Biological Resource Center). The viability of the mouse and human breast cancer cell lines treated with different concentrations of Se NPs was evaluated using the MTT assay after 24 hours. Results depicted in Fig. S50 demonstrated that Se NPs suppressed the proliferation of breast cancer cells in a concentration-dependent manner. Regarding to the mouse breast cancer cells, the inhibitory concentration (IC_{50}) was calculated to be 32.74 μg mL^{-1} for 24 h of exposure. A significant inhibition of cell growth was observed among all treatment groups in a dose-dependent manner. In MCF-7 culture groups, cell survival also decreased with increasing concentration of Se NPs (Fig. S50B). All treatment groups displayed a notable difference in cell viability, except for the group that underwent treatment with 2.5 μg mL^{-1} concentration, which revealed no significant cell mortality compared with the control group. IC_{50} value for the MCF-7 cell line after 24 h was 14.47 μg mL^{-1}. Se NPs also had a significant effect on the viability of MDA-MB-231 cells in all the studied concentrations, and the IC_{50} for these cells after 24 hours of exposure was measured to be 29.39 μg mL^{-1}.

This study evidenced that β-CD@SeNPs can directly induce cell death in cultured mouse and human breast cancer cell lines. β-CD@SeNPs reduced cell viability in two human breast cancer cell lines, namely, MDA-MB-231 and MCF-7, and a mouse derived breast cancer cell line, 4T1. These results were consistent with earlier reports that indicated Se NPs can inhibit cell proliferation and induce apoptosis in cancer cell lines.[35,36] Exposure of 4T1 cells to Se NPs led to a decrease in cell number that was found to be time- and concentration-dependent.

A decrease in viability of MDA-MB-231, MCF-7 and 4T1 cells treated with all concentrations of Se NPs confirmed that the reduction in cell number was due to enhanced cell death. In this study, cells were exposed to DMEM media containing different concentrations of Se NPs. In 4T1 cells, the IC_{50} values for Se NPs were lower than those of human breast cancer cell lines. This phenomenon may be attributed to the varying doubling times of these cells. Research has indicated that cells that proliferate more rapidly tend to exhibit greater sensitivity to anticancer treatments,[37] and 4T1 has the lowest doubling time among the studied cell lines.[38]

Based on our review of the literature on the conversion of SeO_2 to elemental selenium in oxidation processes, we propose a mechanism for the simultaneous synthesis of dialkyl phosphoric acids and selenium nanoparticles through the reaction of dialkyl phosphites and SeO_2, as shown in Scheme 3. Initially, the reaction of SeO_2 with the tautomeric form of dialkyl phosphite gave intermediate **I**, which then underwent an internal oxidative rearrangement, giving intermediate **II**. The next step involved the nucleophilic attack of a dialkyl phosphite on the intermediate **II**, giving intermediate **III** and one molecule of dialkyl phosphoric acid. Finally, elemental selenium and second dialkylphosphoric acid form *via* an internal oxidative rearrangement of the intermediate **III**. ^{31}P NMR spectra at different reaction times showed the complete conversion of the compound **1a** to **2a** in the presence of SeO_2 (Fig. S53).

The oxidative and reductive properties of SeO_2 were initially studied using cyclic voltammetry (Fig. S51). The progress of the chemical reaction of SeO_2 in the presence of diethyl phosphite was then examined by recording consecutive cyclic voltammograms during the reaction. Fig. 4 shows the cyclic voltammograms of 1 mmol diethyl phosphite added to an electrochemical cell containing 0.5 mmol SeO_2 in 10 mL of aqueous solution and 0.1 M KCl in the potential range of 0 to +1.5 V at 100 mV s^{-1}. The waveform of the cyclic voltammograms varied significantly during the progress of the reaction from curve a (at the start of the reaction) to curve i (at the end of the reaction). Obviously, the absence of any anodic signals indicated the non-electroactivity of SeO_2 and diethyl phosphite in the studied range of

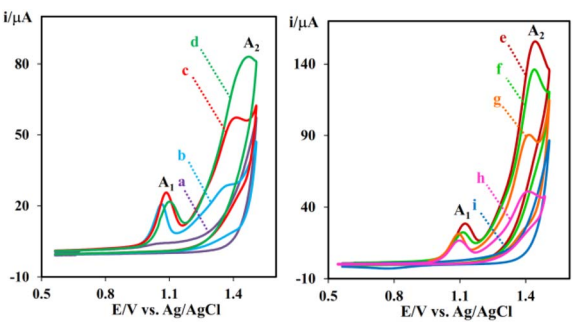

Fig. 4 Cyclic voltammograms (curves of a–i) of SeO_2 (0.5 mmol) in the presence of diethyl phosphite (1 mmol) during the progress of the chemical reaction. The other conditions are the same as Fig. S49 (SI).

potentials. After a while, the colorless solution turned to light-pink, indicating the formation of Se0 nanoparticles. This observation was accompanied with the appearance of two distinct anodic signals of A_1 and A_2, which were related to the oxidation of Se0 and probably an intermediate produced from the chemical reaction, respectively. The height of the A_2 signal was initially increased (from a to e). However, it was gradually decreased (from e to h) and finally disappeared at the end of the reaction (curve i). The data clearly confirmed the connection of the A_2 signal to the intermediate formation. According to Scheme 2, the chemical reaction of SeO_2 and diethyl phosphite resulted in an intermediate **II** with Se^{II}. The anodic A_2 signal was attributed to the oxidation of the Se^{II} center to Se^{IV}. It is worth mentioning that at the end of the reaction, a dense selenium solid was deposited at the bottom of the cell. Therefore, the A_1 peak was omitted at the end of the reaction.

Conclusion

In summary, this study focuses on the simultaneous synthesis of dialkyl phosphoric acids and selenium nanoparticles by a novel, eco-friendly, non-toxic, and sustainable method. The method involves the reaction of dialkyl phosphites with selenium dioxide in water under an optimal condition of 2 : 1 ratio of dialkyl phosphites to selenium dioxide. Dialkyl phosphites act as a reducing agent for converting selenium dioxide to selenium nanoparticles (Se NPs), and conversely, selenium dioxide oxidizes dialkyl phosphites to dialkyl phosphoric acids. Further, the Se NPs are characterized for their morphological and structural features by appropriate advanced analytical methods. TEM analysis suggests that the hemispherical-shaped nanoparticles with smooth surfaces are polydispersed. The reported method presents the synthesis of valuable Se NPs (hemispherical Se crystals) and industrially applicable dialkyl phosphoric acids from inexpensive materials with zero E factor and atom economy. Studies on the anticancer properties of β-cyclodextrin-stabilized Se NPs (β-CD@SeNPs) indicated that cells that proliferate more rapidly tend to exhibit greater sensitivity to anticancer treatments, and 4T1 has the lowest doubling time among the studied cell lines.

Experimental

General methods

All chemicals were commercial products. NMR spectra were obtained using a 400 MHz Bruker Avance instrument, with the chemical shifts being reported as δ ppm and couplings expressed in Hertz. The chemical shift data for each signal on 1H NMR were given in units of δ relative to $CHCl_3$ ($\delta = 7.26$) in $CDCl_3$ solution. For 13C NMR spectra, the chemical shifts in $CDCl_3$ and DMSO were recorded relative to the $CDCl_3$ resonance ($\delta = 77.0$) and DMSO resonance ($\delta = 40.45$). Silica gel column chromatography was carried out with silica gel 100 (Merck No. 10184). Merck silica-gel 60 F254 plates (No. 5744) were used for the preparative TLC.

General procedure for the conversion of dialkyl phosphites to dialkyl phosphoric acids

A solution of selenium dioxide (110 mg, 0.5 mmol) in either water or acetonitrile (4.0 mL) was prepared. Dialkyl phosphites or diaryl phosphine oxide **1** (1.0 mmol) was then added to the solution at room temperature under air. The mixture was stirred for 3 hours, during which a red coloration developed, indicating the formation of selenium nanoparticles. The reaction mixture was allowed to stand for an additional 12 hours to facilitate nanoparticle aggregation and growth. Subsequently, the solution was filtered through a 0.45 μm filter to separate the selenium nanoparticles from the solution. Finally, the filtrate was subjected to thermal treatment at 80 °C to remove the solvent, yielding the final product **2** without further purification.

Conflicts of interest

There are no conflicts to declare.

Data availability

The data supporting this article have been included as part of the Supplementary Information (SI). Supplementary information: details of analytical data of the products and copies of NMRs. See DOI: https://doi.org/10.1039/d5ra04981d.

Acknowledgements

This work was funded by the Iran National Science Foundation (INSF) under project No. 4025386. The authors also gratefully acknowledge support from the Institute for Advanced Studies in Basic Sciences (IASBS). The authors would like to thank Ali Seif from IASBS for the help in graphic designing.

References

1 K. Lovato, P. S. Fier and K. M. Maloney, *Nat. Rev. Chem.*, 2021, **5**, 546–563.
2 M. O. Simon and C. J. Li, *Chem. Soc. Rev.*, 2012, **41**, 1415–1427.
3 M. Cortes-Clerget, J. Yu, J. R. A. Kincaid, P. Walde, F. Gallou and B. H. Lipshutz, *Chem. Sci.*, 2021, **12**, 4237–4266.
4 R. N. Butler and A. G. Coyne, *Chem. Rev.*, 2010, **110**, 6302–6337.
5 S. Kar, H. Sanderson, K. Roy, E. Benfenati and J. Leszczynski, *Chem. Rev.*, 2022, **122**, 3637–3710.
6 K. T. anf F. Toda, *Chem. Rev.*, 2000, **100**, 1025–1074.
7 N. Bisht, P. Phalswal and P. Khanna, *Mater. Adv.*, 2022, **3**, 1415–1431.
8 S. Chhabria, *Encycl. Nanosci. Nanotehnol.*, 2016, **20**, 1–32.
9 U. Tinggi, *Environ. Health Prev. Med.*, 2008, **13**, 102–108.
10 J. Zhang, and J. E. Spallholz, Toxicity of selenium compounds and nano-selenium particles, in *General, Applied and Systems Toxicology*, ed. D. A. Casciano, and S. C. Sahu, John Wiley & Sons, Hoboken, NJ, USA, 2nd edn, 2011, pp. 787–802.

11 N. Baig, I. Kammakakm and W. Falath, *Mater. Adv.*, 2021, **2**, 1821–1871.
12 (*a*) X. Huang, X. Chen, Q. Chen, Q. Yu, D. Sun and J. Liu, *Acta Biomater.*, 2016, **30**, 397–407; (*b*) T. V. Duncan, *J. Colloid Interface Sci.*, 2011, **363**, 1–24.
13 (*a*) S. Sampath, V. Sunderam, M. Manjusha, Z. Dlamini and A. V. Lawrance, *Molecules*, 2024, **29**, 801; (*b*) Y. Huang, E. Su, J. Ren and X. Qu, *Nano Today*, 2021, **38**, 101205.
14 (*a*) Y. Zhang, W. Zheng, W. Liu, T. Chen, W. Cao, X. Li and Y.-S. Wong, *ACS Nano*, 2012, **6**, 6578–6591; (*b*) L. Kong, Q. Yuan, H. Zhu, Y. Li, Q. Guo, Q. Wang, X. Bi and X. Gao, *Biomaterials*, 2011, **32**, 6515–6522.
15 G. Guisbiers, H. H. Lara, R. Mendoza-Cruz, G. Naranjo, B. A. Vincent, X. G. Peralta and K. L. Nash, *Nanomedicine*, 2017, **13**, 1095–1103.
16 S. C. Singh, S. K. Mishra, R. K. Srivastava and R. Gopal, *J. Phys. Chem. C*, 2010, **114**, 17374–17384.
17 (*a*) W.-Y. Tzeng, Y.-H. TsengT, T. Yeh, C. –M. Tu, R. Sankar, Y.-H. Chen, B.-H. Huang, F.-C. Chou and C.-W. Luo, *Opt. Express*, 2020, **28**, 685–694; (*b*) M. Quintana, E. Haro-Poniatowski, J. Morales and N. Batina, *Appl. Surf. Sci.*, 2002, **195**, 175–186.
18 B. T. Mayers, K. Liu, D. Sundewrland and Y. Xia, *Chem. Mater.*, 2003, **15**, 3852–3858.
19 V. Cittrarasu, D. Kaliannan, K. Dharman, V. Maluventhen, M. Easwaran and W. C. Liu, *Sci. Rep.*, 2021, **11**, 1032.
20 B. Kaboudin, P. Daliri, S. Faghih and H. Esfandiari, *Front. Chem.*, 2022, **10**, 890696.
21 M. Vandevelde, A. Simoens, B. Vandekerckhove and C. Stevens, *RSC Med. Chem.*, 2024, **15**, 998–1002.
22 R. Murugavel, A. Choudhury, M. G. Walawalkar, R. Pothiraja and C. N. Rao, *Chem. Rev.*, 2008, **108**, 3549–3655.
23 (*a*) K. W. Smith, and L. J. Persinski, 5417287, *US Pat.*, 1995; (*b*) K. W. Smith and L. J. Persinski, *Chem. Abstr.*, 1995, **123**, 87963.
24 Z. Cai, X. Zeng, Y. Zhang, Y. Liu, G. Tang, Y. Zhao and A. Synyt, *Catal*, 2022, **364**, 2916–2921.
25 M. M. Ali, M. H. Taha and H. M. Killa, *J. Radioanal. Nucl. Chem.*, 2014, **300**, 963–967.
26 S. Tachimori, B. Krooss, H. Nakamura and J. Radioanal, *Chem*, 1978, **43**, 53–63.
27 (*a*) R. A. Aithken, C. J. Colett and S. T. E. Masher, *Synthesis*, 2012, **44**, 2515–2518; (*b*) S. T. Mesher, C. Collett, *PCT Int. Appl. WO 2010/022496*, 2010; (*c*) S. T. Mesher and C. Collett, *Chem. Abstr.*, 2010, **152**, 339215.
28 (*a*) P.-L. Wu, J.-H. Chen and D.-S. Huang, *J. Chin. Chem. Soc.*, 1999, **46**, 967; (*b*) P.-L. Wu, J.-H. Chen and D.-S. Huang, *J. Chem., Abstr.*, 2000, **132**, 166275.
29 A. Krief, and L. Hevesi, Selenium Dioxide Oxidations, in *Organoselenium Chemistry I*, Springer, Berlin, Heidelberg, 1988, 115–180.
30 B. Kaboudin, S. Alaie and T. Yokomatsu, *Tetrahedron: Asymmetry*, 2011, **22**, 1813–1816.
31 A. G. Kannan, N. R. Choudhury and N. K. Dutta, *Polymer*, 2007, **48**, 7078–7086.
32 J. F. Moulder, W. F. Stickle, P. E. Sobol, K. Bomben, and J. Chastain, Handbook of X-ray photoelectron spectroscopy, in *Perkin-Elmer Corporation, Physical Electronics Division*, ed. M. N. Eden Prairie, 2nd edn, 1992, p. 216–232.
33 M. Pelavin, D. Hendrickson, J. Hollander and W. Jolly, *J. Phys. Chem.*, 1970, **74**, 1116–1121.
34 B. Kaboudin, B. Burunli, M. Nazerian, T. Zhang and Y. Gu, *J. Organomet. Chem.*, 2025, **1025**, 123477.
35 E. G. Varlamova, I. V. Baimler, S. V. Gudkov, et al., *Appl. Sci.*, 2023, **13**, 10763.
36 T. H. D. Nguyen, B. Vardhanabhuti, M. Lin and A. Mustapha, *Food Control*, 2017, **77**, 17–24.
37 A. Khosravi and J. Asadi, *Med. Lab. J.*, 2021, **15**, 23–27.
38 T. Kremmer, I. Pälyi, D. Daubner, M. Boldizsar, B. Vincze, E. Paulik, J. Sugar, E. Pokorny and E. Tury, *Anticancer Res.*, 1991, **11**, 1807–1813.